Cell

External Lipid PI3P Mediates Entry of Eukaryotic Pathogen Effectors into Plant and Animal Host Cells

Shiv D. Kale,[1] Biao Gu,[1,2] Daniel G.S. Capelluto,[3] Daolong Dou,[1,5] Emily Feldman,[1] Amanda Rumore,[1,3] Felipe D. Arredondo,[1] Regina Hanlon,[1] Isabelle Fudal,[4] Thierry Rouxel,[4] Christopher B. Lawrence,[1,3] Weixing Shan,[2,*] and Brett M. Tyler[1,*]

[1]Virginia Bioinformatics Institute, Virginia Polytechnic Institute and State University, Blacksburg, VA 24061, USA
[2]College of Plant Protection and Shaanxi Key Laboratory of Molecular Biology for Agriculture, Northwest A & F University, Yangling, Shaanxi 712100, China
[3]Department of Biological Sciences, Virginia Polytechnic Institute and State University, Blacksburg, VA 24061, USA
[4]INRA-Bioger, Campus AgroParisTech, 78850 Thiverval-Grignon, France
[5]Present address: Department of Plant Pathology, Nanjing Agricultural University, Nanjing 210095, China
*Correspondence: wxshan@nwsuaf.edu.cn (W.S.), bmtyler@vt.edu (B.M.T.)
DOI 10.1016/j.cell.2010.06.008

SUMMARY

Pathogens of plants and animals produce effector proteins that are transferred into the cytoplasm of host cells to suppress host defenses. One type of plant pathogens, oomycetes, produces effector proteins with N-terminal RXLR and dEER motifs that enable entry into host cells. We show here that effectors of another pathogen type, fungi, contain functional variants of the RXLR motif, and that the oomycete and fungal RXLR motifs enable binding to the phospholipid, phosphatidylinositol-3-phosphate (PI3P). We find that PI3P is abundant on the outer surface of plant cell plasma membranes and, furthermore, on some animal cells. All effectors could also enter human cells, suggesting that PI3P-mediated effector entry may be very widespread in plant, animal and human pathogenesis. Entry into both plant and animal cells involves lipid raft-mediated endocytosis. Blocking PI3P binding inhibited effector entry, suggesting new therapeutic avenues.

INTRODUCTION

Pathogens of both plants and animals produce effectors and/or toxins that act within the cytoplasm of host cells to suppress host defenses and cause disease (Bhavsar et al., 2007; Chisholm et al., 2006; Lafont et al., 2004; Tyler, 2009). Many bacterial pathogens use specialized secretion machineries to directly inject effectors into host cells (Tseng et al., 2009). In addition, many bacterial toxins can enter host cells by receptor-mediated endocytosis after binding glycolipid receptors (Lafont et al., 2004). Apicomplexan parasites such as *Plasmodium* that are enclosed within a parasitiphorous vacuole employ a host targeting signal (HTS), that includes the Pexel motif, to target secreted effectors for translocation across the parasitiphorous vacuolar membrane (Hiller et al., 2004; Marti et al., 2004; Bhattacharjee et al., 2006). Effectors from oomycete plant pathogens carry an HTS, containing RXLR and dEER motifs (Rehmany et al., 2005; Tyler et al., 2006; Jiang et al., 2008), that can translocate them into host cells in the absence of the pathogen (Dou et al., 2008; Whisson et al., 2007), but the mechanism of translocation was not identified. Oomycetes are fungus-like relatives of marine algae that cause many destructive plant diseases, such as potato late blight that caused the Irish potato famine in the nineteenth century (Tyler, 2007).

Effectors of fungal plant pathogens have also been predicted to translocate into host cells because many plants possess intracellular receptors, encoded by major resistance (R) genes, that mediate a rapid defense response when fungal effectors are present (Ellis et al., 2006; Tyler, 2002). For example, the R genes *L5*, *L6* or *L7* of flax (*Linum usitatissimum*) mediate a rapid defense response against lines of the flax rust fungus *Melampsora lini* that produce the effector AvrL567 (Ellis et al., 2007). Like many plant R genes, *L5*, *L6* and *L7* encode intracellular proteins with nucleotide binding sites and leucine-rich-repeats (NBS-LRR proteins) (Ellis et al., 2007). The L6 protein can bind directly to AvrL567 and binding is necessary to trigger a defense response (Ellis et al., 2007). Thus, AvrL567 is inferred to possess a mechanism to cross the flax plasma membrane. Fungal effectors with intracellular targets can also be found in wilt pathogens such as *Fusarium oxysporum* f.sp. *lycopersici* (*Fol*); the Avr2 effector of this tomato pathogen is found in the xylem but interacts with an NBS-LRR *R* gene product, I-2, in the host cytoplasm (Houterman et al., 2009). Furthermore, effectors of the rice blast fungus, *Magnaporthe oryzae* could be observed to enter rice cells from the pathogen (Khang et al., 2010). In the case of oomycetes, there are many plant NBS-LRR-class *R* genes that confer resistance against these pathogens, and in several cases an RXLR-dEER effector targeted by one of these *R* genes has been identified (Tyler, 2009). Examples include *Phytophthora sojae* effector Avr1b targeted by soybean *Rps*1b (Shan et al., 2004) and *P. infestans* effector Avr3a targeted by potato *R*3a

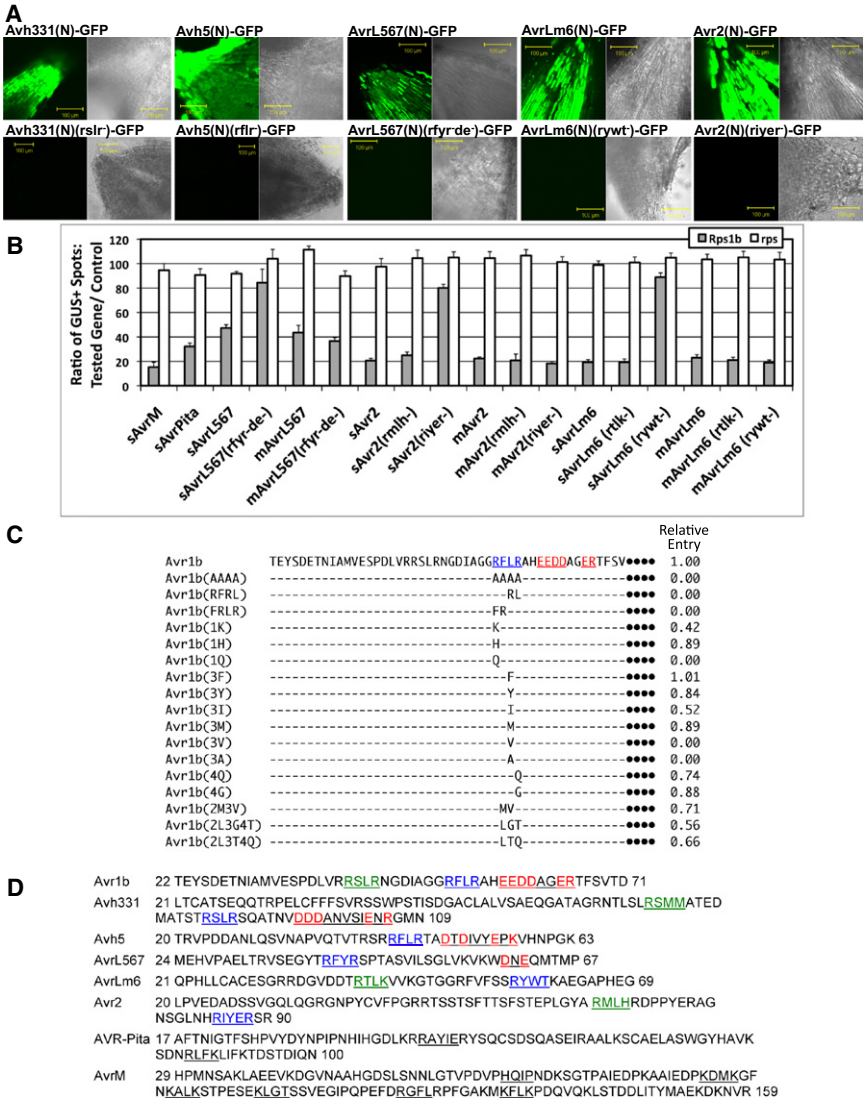

Figure 1. Identification of Motifs Mediating Cell Entry by Fungal Effectors

(A) Entry of wild-type and mutant effector-GFP fusion proteins into soybean root cells. Root tips were incubated with protein (1 mg/mL) for 12 hr, then washed for 2 hr. See also Figure S1 and Table S2.

(B) Double-barrel particle bombardment cell re-entry assays of fungal effectors fused to Avr1b. N-terminal sequences of each effector were fused to the C-terminal domain of Avr1b with (s) or without (m) the Avr1b secretory leader. Effector re-entry into soybean leaf cells resulting in cell killing was measured in the presence or absence of resistance gene *Rps*1b. Averages and standard errors shown. See also Table S1.

(C) Mutations of the Avr1b RXLR motif assayed using the double barrel particle bombardment assay. Cell entry activity measured as cell death in the presence of Rps1b relative to wild-type Avr1b. Dashes indicate identical residues; •••• indicates Avr1b sequences. Data for AAAA, RFRL, FRLR, 1K, 1Q, and 4Q mutants from Dou et al., (2008).

(D) Sequence of the cell entry domains of the effectors analyzed in (A) and (B). Active and inactive RXLR-like motifs are underlined in blue and green respectively, predicted RXLR-like motifs of unknown function are underlined in black; dEER motifs are underlined with the predicted active residues in red. Two predicted motifs in Avr-Pita overlap (RLFK and KLIF).

(Armstrong et al., 2005). Genes that encode effectors targeted by *R* gene products have historically been called avirulence genes because expression of the effector prevents infection when the plant host contains the cognate *R* gene (Jones and Dangl., 2006).

We show here that in order to carry effectors into host cells, oomycete RXLR-dEER host-targeting signals, and similar signals in fungal effectors, bind to host cell surface phosphatidylinositol-3-phosphate (PI3P).

RESULTS

Identification of Fungal Effector Translocation Motifs

The RXLR-dEER domain of *P. sojae* Avr1b enables translocation of green fluorescent protein (GFP) into plant cells without any pathogen-encoded machinery (Dou et al., 2008). The same is true for full-length Avr1b protein and for two additional bioinformatically predicted effectors, Avh5 and Avh331, based on uptake of effector-GFP fusion proteins into soybean root cells (Figure 1A and Figures S1A–S1J available online) and on re-entry of Avh331 protein after expression and secretion from soybean leaf cells following particle bombardment (Dou et al., 2008; Kale and Tyler, 2009) (Table S1). As in the case of Avr1b, both the RXLR and the dEER motifs of Avh5 and Avh331 (Figure 1D) were required for cell entry in the GFP root uptake assay (Figure 1A and Figures S1I and S1J) and the leaf bombardment assay (Table S1). To test whether fungal effectors contain N-terminal cell entry domains, we fused N-terminal segments from the fungal effectors AvrL567 from *M. lini* (Ellis et al., 2007), Avr2 from *Fol* (Houterman et al., 2009) and AvrLm6 from *Leptosphaeria maculans* (Fudal et al., 2007) to GFP. When the fusion proteins were incubated with soybean roots, strong accumulation of the proteins was observed in the root cells (Figure 1A), including the nuclei (Figures S1Q–S1S). The leaf bombardment assay confirmed that the N-terminal segments of all three fungal effectors could deliver Avr1b back into soybean leaf cells following secretion (Figure 1B), as could the N-terminal domains of AvrM from *M. lini* (Ellis et al., 2007) and of AVR-Pita from *M. oryzae* (Jia et al., 2000) (Figure 1B).

Since the fungal effectors contained no obvious RXLR or dEER motifs, we used the leaf bombardment assay to define the range of residues within the RXLR motif of Avr1b that could permit cell entry. The results (Figure 1C) revealed that lysine or histidine but not glutamine could replace the arginine at position 1 in the motif,

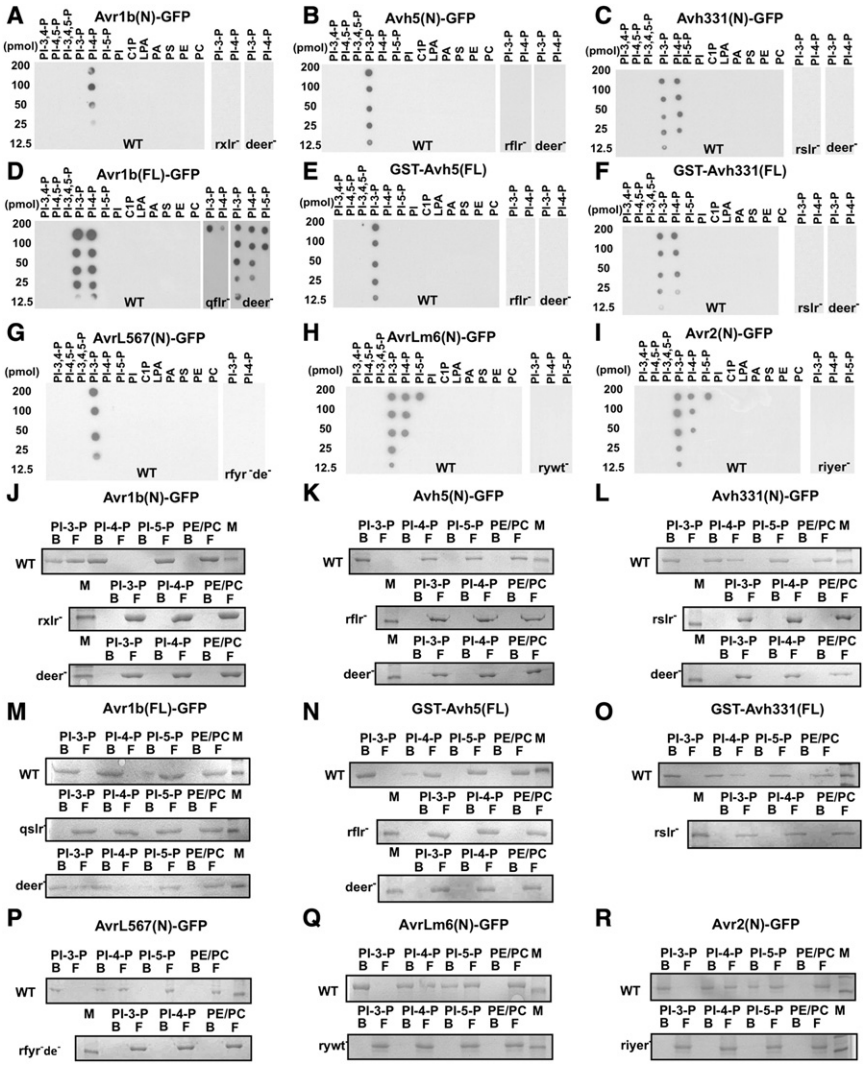

Figure 2. Binding of Oomycete and Fungal Effector Proteins to Phosphoinositides

(A–I) Filter-binding assays.

(J–R) Liposome-binding assays.

(N)-GFP and (FL)-GFP indicate a fusion of the N-terminal domain of an effector or the full-length protein, respectively, to the N terminus of GFP. GST-XXX(FL) indicates a fusion of a full-length effector protein (without signal peptide) to the C terminus of GST. PI-3,4-P = phosphatidylinositol-3,4-bisphosphate; PI-4,5-P = phosphatidylinositol-4,5-bisphosphate; PI-3,4,5-P = phosphatidylinositol-3,4,5-triphosphate; PI-3-P = phosphatidylinositol-3-phosphate; PI-4-P = phosphatidylinositol-4-phosphate; PI-5-P = phosphatidylinositol-5-phosphate; PI = phosphatidylinositol; C1p = ceramide-1-phosphate; LPA = lysophosphatidic acid; PA = phosphatidic acid; PS = phosphatidylserine; PE = phosphatidylethanolamine; PC = phosphatidylcholine. Except where shown, no mutant proteins bound to PI-3,4-P, PI-4,5-P, PI-3,4,5-P, PI-5-P, PI, C1P, LPA, PA, PS, PE, or PC (Figure S2). In the liposome binding assays (right panels), "B" and "F" indicate liposome-bound and -free proteins, respectively; "M" = size markers.

See also Figure S2.

that any large hydrophobic residue (isoleucine, methionine, phenylalanine, or tyrosine) could replace the leucine at position 3, but valine and alanine could not. At position 4, all residues tested allowed function. Furthermore, the presence of either an leucine or methionine residue at position 2 could substitute for leucine at position 3.

Using this information, we identified potential cell entry motifs in the N-terminal regions of the five fungal effectors (Figure 1D). A single motif in AvrL567, RFYR, was a close match to the oomycete RXLR motif. Alanine substitutions in the RFYR motif (Figure 1D) abolished the activity of the AvrL567 N-terminal domain in the leaf bombardment assay; when fused to Avr1b, cell killing in the presence of *Rps*1b was dependent on an intact RFYR motif, but only when the secretory leader was present (Figure 1B). When the alanine substitutions were introduced into the AvrL567(N)-GFP fusion protein, the protein did not accumulate in root cells (Figure 1A).

Substitution mutations were also introduced separately into two candidate cell entry motifs in each of AvrLm6 (RTLK and RYWT) and Avr2 (RMLH and RIYER). The mutations in the RYWT motif of AvrLm6 and in the RIYER motif of Avr2 abolished effector-GFP accumulation in root cells (Figures 1A and S1) and re-entry in the bombardment assay (Figure 1B). However the mutations in the RTLK motif of AvrLm6 and the RMLH motif of Avr2 had no measurable effect in either assay (Figure 1B and S1K,L). Mutations in the individual candidate motifs of AvrM and AVR-Pita had no effect on cell entry as measured by the bombardment assay (data not shown), indicating either that none of the candidates were involved in cell entry, or that each effector contained more than one functional motif.

Oomycete RXLR-dEER Domains Bind Phosphoinositides

In principle, a cell entry domain could bind either a (glyco)protein or (glyco)lipid receptor. After noting that beta-type phosphatidylinositol-4-phosphate (PI4P) kinases from rice and *Arabidopsis* contained PI4P binding domains that consisted of tandem repeats containing RXLR-dEER-like motifs (Lou et al., 2006), we tested whether oomycete RXLR-dEER domains could bind phosphoinositides. Thirteen lipids were spotted onto a membrane, which was probed with GFP fused to the N-terminal RXLR-dEER domains of Avr1b, Avh331 or Avh5, or to full-length Avr1b [Avr1b(FL)]. The Avr1b(FL)- and Avh331(N)-GFP fusions bound to both PI3P and PI4P (Figures 2C and 2D) while Avh5 (N)-GFP fusions bound mostly to PI3P (Figure 2B). The Avr1b N-terminus bound mostly to PI4P (Figure 2A); presumably this small difference in specificity arises from changes in the structure

of the N-terminus in the absence of the rest of the protein. No other phospholipids were bound, including PI5P, phosphatidylinositol-polyphosphates, or other anionic phospholipids. Substitution mutations in the RXLR or dEER motifs that abolished entry into soybean root and leaf cells (Dou et al., 2008; Figure 1 and Figure S1) also abolished binding, including interchanges of amino acids of the RXLR motif of Avr1b that preserved the positive charge (RFLR- > FRLR or RFLR- > RFRL) (Figure S2A). One exception was the dEER mutant of Avr1b which abolished binding only in the context of the N-terminal domain, suggesting a second redundant dEER-like motif further downstream. Fusions of full-length Avh5 or Avh331 proteins to the C terminus of glutathione S-transferase (GST) could also bind the same phosphoinositides as the N-terminal GFP fusions (Figures 2E and 2F). GST and GFP proteins alone did not bind any lipids (Figure S2A). Alanine substitutions in the RXLR or dEER motifs of full-length Avh5 proteins did not alter their far-UV circular dichroism spectra compared to wild-type Avh5, indicating that the substitutions did not significantly disturb the global fold of the effector protein (Figure S1T and Table S2).

To independently confirm binding of the RXLR-dEER domains to phosphoinositides, we tested the binding of the fusion proteins to liposomes composed of phosphatidylcholine (PC) and phosphatidylethanolamine (PE). None of the effector-GFP or GST-effector fusion proteins bound to liposomes (Figures 2J–2O and Figure S2B). However, when either PI3P or PI4P was included, all the fusion proteins bound to the liposomes. In every case, when any of the RXLR or the dEER motifs were mutated, the mutant fusion proteins lost their ability to bind to liposomes (Figures 2J–2O and Figure S2B) except for the dEER mutant of Avr1b(FL) which retained weak binding to several PI-Ps.

Fungal Effectors Also Bind Phosphoinositides

Both filter binding and liposome binding were used to test whether the N-terminal domains of AvrL567, AvrLm6, and AvrLm2 bound phosphoinositides. Figures 2G–2I show that all three fusions could bind PI3P, and more weakly to PI4P and/or PI5P (Figures 2G–2I and 2P–2R). Mutations in the functional RXLR-like motifs of each effector resulted in a loss of binding (2G–2I and 2P–2R) while mutations in the nonfunctional RXLR-like motifs of AvrLm6 and Avr2 did not affect binding (Figure S2). The host-targeting signals (HTS) of three *Plasmodium falciparum* effectors, PfGBP, PfHRPII, and Pf1615c, could carry Avr1b into plant cells (Dou et al., 2008; Figure S1M). The HTS regions of PfHRPII (Figure S2B) and the other two effectors (not shown) also could bind PI3P and/or PI4P, and the binding required intact pexel motifs.

PI3P Is Present on the Outer Surface of Plant and Human Cell Plasma Membranes

In order to test which, if any, phosphoinositide was present on the outer surface of plant cells, we created highly specific biosensors for PI3P and PI4P by fusing the PH domains of the human proteins PEPP1 and FAPP1 (Dowler et al., 2000; Vermeer et al., 2009) to GFP and to mCherry (Figure S3A). We also fused GFP to the PX domain of VAM7p, which binds preferentially to PI3P (Lee et al., 2006). Finally, we employed GFP and mCherry biosensors containing two tandem repeats of the PI3P-specific FYVE domain of the rat Hrs protein (Hrs-2xFYVE) (Vermeer et al., 2006). Each protein was incubated with soybean root suspension culture cells (Figure 3A) or with soybean roots (Figure 3B) and then the cells were subjected to plasmolysis to separate the plasma membranes from the cell walls. All three of the PI3P-GFP biosensors bound strongly and quite uniformly to the plasma membrane of the suspension and root cells, whereas no binding was observed to the PI4P biosensor FAPP1-PH-GFP. Figures 3E and 3F show that all four of the biosensor proteins showed the expected binding specificity.

Phosphatidylinositol phosphates are universally found in eukaryotic cells. Since a number of human and animal diseases are caused by fungi and oomycetes, we tested the possibility that cell surface PI3P or PI4P might be available to mediate effector protein entry into animal cells, using the human lung epithelial cell line A549 as a model. At 2°C, which inhibits endocytosis, all three of the PI3P-GFP biosensors bound strongly to the plasma membrane of the A549 cells, but no binding was observed to the PI4P biosensor (Figures 3C and 3D). In contrast to the root cells, binding to the surface of A549 cells was highly punctate. Since there are numerous reports that erythrocytes do not have cell surface phosphoinositides (reviewed in Quinn, 2002; Boon and Smith, 2002), we tested the binding of the four biosensors to human erythrocytes. No binding was observed to the erythrocytes by any of the biosensors nor by any effector GFP fusions (Figure 3D), which is in agreement with the literature, but which suggests that there may be differences among animal cell types with regard to the presence of outer surface phosphoinositides.

Inhibition of Effector Entry by PI3P Binding Proteins and Exogenous Inositol Phosphates

To test the hypothesis that the fungal and oomycete effectors bound external PI3P in order to enter plant cells, we incubated the effector-GFP fusions with the roots in the presence of a molar excess of each of the PI3P- and PI4P-binding biosensor proteins. All three PI3P-binding proteins completely abolished entry by the four effector-GFP fusions (Avr1b, AvrL567, AvrLm6 and Avr2) into soybean root cells (Figures 4A–4D, rows 2–4). In contrast, FAPP1-PH-mCherry did not inhibit uptake of any of the effector-GFP fusions (Figures 4A–4D, row 5), consistent with the hypothesis that PI3P, but not PI4P, is required for effector entry.

A synthetic cell entry motif composed of nine-arginine residues (Arg_9) was previously shown to deliver Avr1b and GFP into plant cells (Dou et al., 2008; Chang et al., 2005). The Arg_9-GFP fusion protein binds PI3P, PI4P, PI-polyphosphates and PS, albeit weakly in each case (Figure S4C). Figure 4E shows that none of the four biosensor proteins could inhibit the uptake of Arg_9-GFP, confirming that the PI3P biosensors did not cause a generalized inhibition of protein uptake.

To further confirm the role of PI3P binding in effector cell entry, we utilized inositol-1,3-diphosphate (1,3IP2) and inositol-1,4-diphosphate (1,4IP2); these compounds represent the hydrophilic head-groups of PI3P and PI4P, respectively, and thus were potential competitive inhibitors of effector binding. Preincubation with 100 μM 1,3IP2 inhibited binding of all the

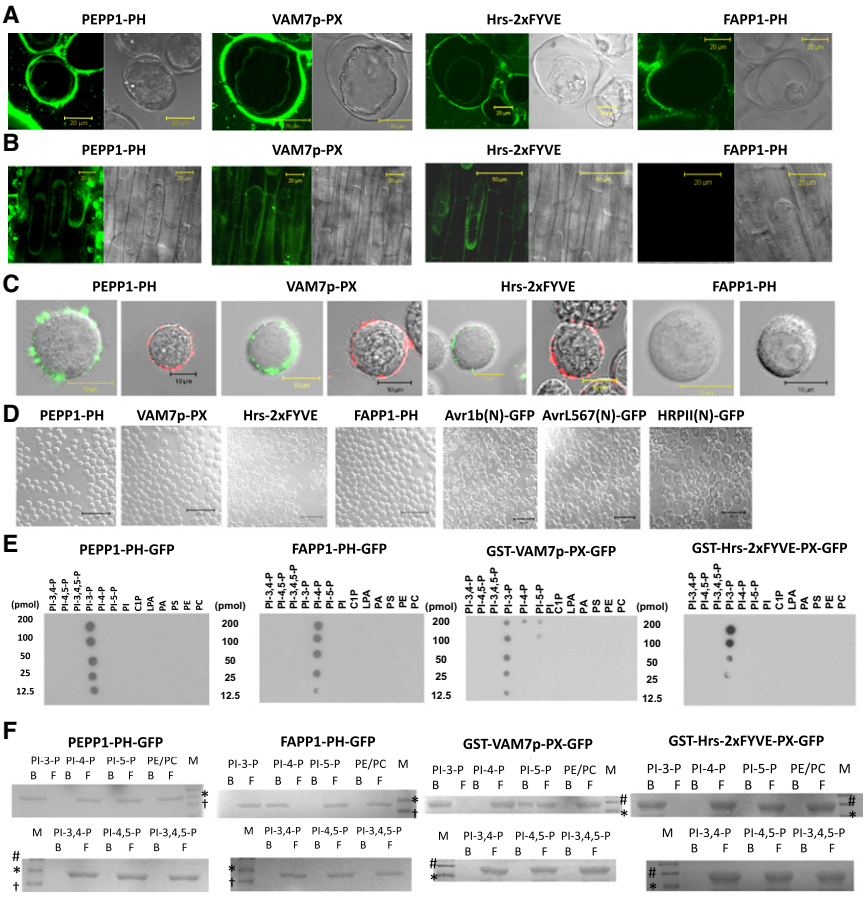

Figure 3. PI3P Occurs on the Outer Surface of Soybean Root Cells and Human Epithelial Cells

(A and B) Soybean root suspension culture cells (A) or root tips (B) incubated with GFP biosensors for 6 hr (A) or 12 hr (B) at 2°C, washed for 2 hr, then plasmolyzed with 0.8M Mannitol (A) or 4M NaCl (B) for 30 min. Left panels, fluorescence images; right panels, light micrographs. The scale bars represent 20 μm or 50 μm, respectively.

(C) A549 epithelial cells incubated with GFP biosensors (left panels) or mCherry biosensors (right panels) for 6 hr at 2°C, then washed twice briefly. Light micrographs are overlaid with fluorescence images. The scale bar represents 10 μm.

(D) Human erythrocytes incubated with GFP biosensors (panels 1-4) or effector-GFP fusions (panels 5–7) for 6 hr at 2°C, then washed twice briefly. Light micrographs are overlaid with fluorescence images. The scale bar represents 20 μm.

(E and F) Lipid blots (E) and liposome binding assays (F) validating the specificity of the biosensor proteins. Details as described in Figure 2. See also Figure S3.

effector-GFP fusions to PI3P-containing liposomes (Figure S4B). 1,4IP2 (100 μM) also inhibited binding to PI3P in every case, indicating that the specificity of binding was relaxed in the case of the soluble head group compounds. In concert with this observation, both 1,3IP2 and 1,4IP2 (500 μM) could completely inhibit root cell entry when preincubated with each of the effector fusions for 30 min prior to exposure to soybean roots (Figure 4A–4D, rows 6 and 7). Neither 1,3IP2 nor 1,4IP2 could inhibit the binding of Arg_9-GFP to liposomes (Figure S4B) and accordingly, uptake of Arg_9-GFP was unaffected by preincubation with either 1,3IP2 or 1,4IP2 (Figure 4E), confirming that neither compound caused a generalized inhibition of protein uptake.

As a further test of the ability of PI3P-binding proteins and IP2 to block effector entry into plant cells, full-length Avr1b protein and full-length Avh331 protein were infiltrated into soybean leaves containing the *Rps*1b or *Rps*1k resistance genes, respectively. As previously shown (Shan et al., 2004), Avr1b protein triggers programmed cell death (PCD) when infiltrated into *Rps*1b leaves (Figure 4F). As expected, no PCD was triggered when RXLR or dEER motif mutations were present (Figure S4A) or *Rps*1b was absent (Figure 4F). Avh331 is a candidate product of the *Avr1k* gene, and triggers programmed cell death (PCD) in *Rps*1k leaves when expressed in the leaf cells following particle bombardment, but not in leaves lacking *Rps*1k (Table S1). As predicted therefore, full-length Avh331 protein triggered PCD when infiltrated into *Rps*1k leaves but not when infiltrated into leaves lacking *Rps*1k (Figure 4G). Furthermore, infiltration of Avh331 protein containing an RXLR mutation did not trigger PCD (Figure S4A).

As shown in Figures 4F and 4G, 1,3IP2, 1,4IP2, and all three of the PI3P-binding proteins, but not the PI4P binding protein, strongly inhibited Rps1b- and Rps1k-mediated PCD when coinfiltrated with Avr1b or Avh331 protein, respectively.

Effector Entry into Human Cells

Given the presence of PI3P on the outside of the A549 human lung epithelial cells, we tested if RXLR-dEER motifs could mediate entry of effector proteins into these cells. GFP fusions with Avr1b and AvrL567 could enter A549 cells (Figures 5A and 5B) as could PfHRPII (from *Plasmodium*) (Figure S5V), and entry required intact RXLR or Pexel motifs (Figures 5A and 5B and Figure S5V). Localization of the GFP fusions inside the cells was confirmed by the accumulation of GFP within vesicle-like structures, and by the fact that the cells were treated with protease (trypsin) prior to photographing. Protein accumulation was strongly inhibited in each case by competing PI3P-binding proteins (which entered the cells instead) or by 1,3IP2 or 1,4IP2, but not by the PI4P mCherry biosensor (Figures 5A and 5B). No effector entry into erythrocytes was observed (Figure 3E), consistent with the absence of PI3P or PI4P from the outer surface of erythrocytes.

Arg9-GFP could also enter the A549 cells, but GFP itself could not (Figure 5C). Entry of Arg9-GFP was not inhibited by1,3IP2, 1,4IP2 or by PI3P- or PI4P-binding proteins, confirming that none of those inhibitors interfered generally with protein uptake by the A549 cells.

To determine if the effector-GFP fusions bound to the same sites on the cells as the PI3P-binding proteins, equimolar

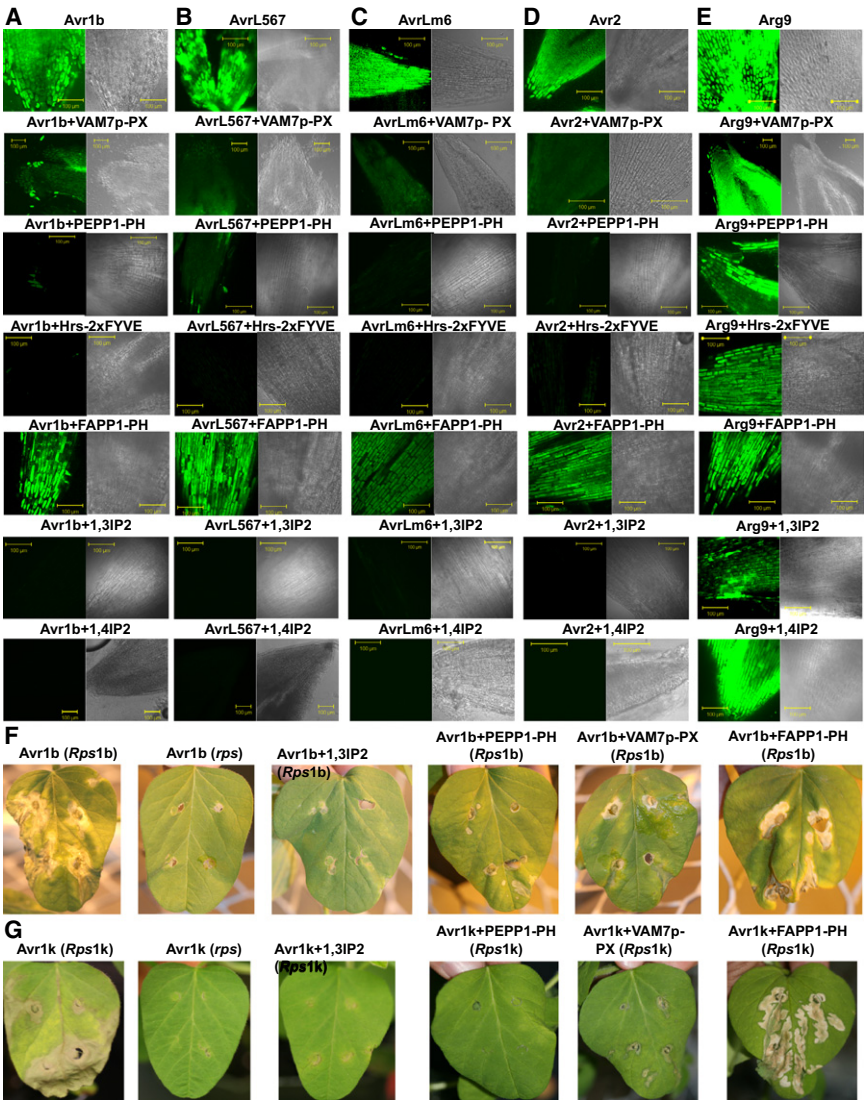

Figure 4. Inhibition of Effector Entry into Plant Cells by PI3P-Binding Proteins and Inositol Diphosphates

(A–E) Inhibition of effector-GFP entry into root cells. In each case, 1 mg/mL effector-GFP protein was incubated with soybean root tips for 12 hr then washed for 2 hr. For biosensor inhibition assays (rows 2–5), root tips were preincubated for 3 hr at room temperature in 5 mg/ml biosensor protein prior to addition of effector-GFP fusion proteins (final concentrations 2.5 mg/mL biosensor, 1.0 mg/mL effector). VAM7p-PX = PX domain alone, with no fluorescent protein fusion; PEPP1-PH, FAPP1-PH, and Hrs-2xFYVE biosensors were all mCherry fusions. For IP2 inhibition assays (rows 6 and 7) 500 μM 1,3IP2 or 1,4IP2 were preincubated with the effector-GFP proteins for 30 min prior to exposure to the roots. The scale bar represents 100 μm. See also Figures S4B and S4C.

(F and G) Inhibition of programmed cell death triggered by entry of Avr1b(FL) (F) and Avh331(FL) (G) into cells of soybean leaves containing cognate resistance genes. 0.25 mg/mL of each protein, lacking N-terminal or C-terminal fusions, were infiltrated into the primary unifoliate leaves from cultivars with no Rps gene (*rps*), *Rps*1b or *Rps*1k. Where indicated, the protein was coinfiltrated with 500 μM 1,3IP2 or with 1.0 mg/ml of the indicated biosensor protein (same biosensors as A-E, except that VAM7p-PX-mCherry was used instead of VAMp7-PX alone). The plant leaves were photographed 5 days after infiltration. See also Figure S4A.

concentrations of the biosensors and effectors were incubated with A549 cells at 2°C. The effector fusions colocalized with each biosensor in a punctate pattern on the surface of the cells (Figures 5D, 5F, and 5H and Figure S5). At 37°C, the three biosensors and the effector fusions were colocalized inside the cells within endosome-like structures (Figures 5E, 5G, and 5I). To support that the proteins were accumulating within endosome-like structures, the A549 cells were stained with FM4-64, a dye that binds to plasma membranes and then, following endocytosis, stains endosomes. The cells were washed and photographed after only 2.5 min, in order to observe the earliest events during entry. Figures 5J–5L shows that the Avr1b-GFP and AvrL567-GFP fusions accumulated within small endosome-like bodies and these bodies were stained with FM4-64.

To further characterize the binding of Avr1b and AvrL567 to the A549 cells, we measured the dissociation constants (K_d) for binding of Avr1b and AvrL567 to the surface of the cells; these were 190 ± 30 nM (standard error) and 330 ± 40 nM respectively (Figure 6A). The K_d's for binding of each effector to PI3P-containing liposomes were very similar, 210 ± 20 nM and 740 ± 120 nM respectively (Figure 6B). Measurements of binding by Avr1b and AvrL567 agreed that the number of PI3P molecules on the surface of each cell averaged 1.4 ± 0.1 × 10^8 (Figure 6A), which equates roughly to 1% of the plasma membrane outer leaflet lipid. The inhibition constants (K_i) for 1,3IP2 inhibition of binding to cells were 16 ± 1.6 μM for Avr1b and 13 ± 0.6 μM for AvrL567 (Figure 6C). The inhibition constants for 1,3IP2 inhibition of binding to PI3P-containing liposomes were of the same order, 1.9 ± 0.1 μM for Avr1b and 7.9 ± 0.7 μM for AvrL567 (Figure 6D).

Effector Cell Entry Is Inhibited by PI3P Depletion and by Inhibitors of Lipid Raft-Mediated Endocytosis

Quantitating the dynamics of effector-GFP accumulation revealed that the fusion proteins accumulated very rapidly, within 2.5 min of exposure to the A549 cells. Over the next hour however, the accumulated fluorescence declined steeply, before slowly recovering over the next 3 hr (Figure 6E). This pattern was also observed for GFP-biosensors and mCherry-biosensors and for Arg_9-GFP. A possible interpretation of this pattern is that the initial massive entry of binding proteins

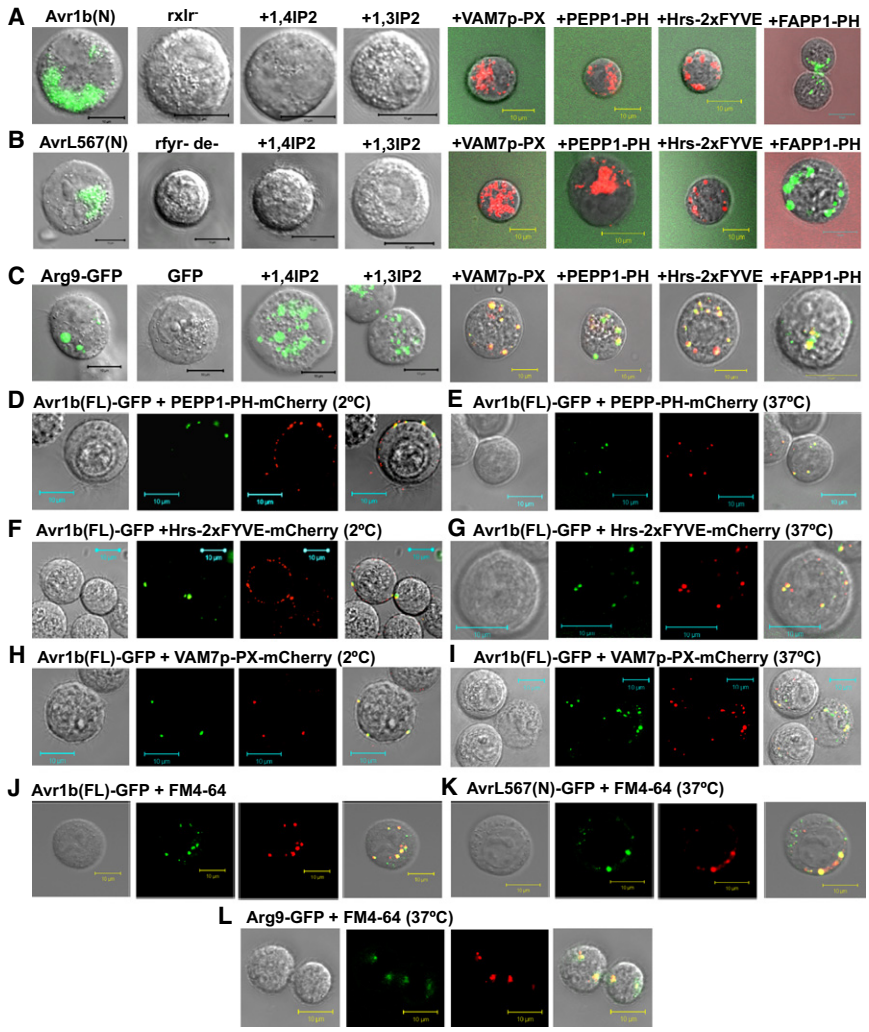

Figure 5. Effector Entry into Human Cells and Inhibition by Inositol Diphosphates and PI3P-Binding Proteins

(A–C) Human A549 cells were incubated with the indicated effector-GFP fusion proteins (25 μg/mL) for 8 hr, in the presence or absence of 500 μM inositol 1,3 diphosphate (1,3IP2), 520 μM inositol 1,4 diphosphate (1,4IP2), or 100 μg/ml of the indicated biosensor protein (mCherry fusion in each case), then washed either twice (panels 1–4) or once (panels 5–8) and photographed. Light micrographs are overlaid with fluorescence images (both red and green channels in panels 5–8). In panels 5–8, traces of the nonentering proteins can be observed in the background. The scale bars represent 10 μm. See also Figure S5.

(D–I) Colocalization of Avr1b(FL)-GFP with mCherry biosensor proteins on the surface (D, F, and H) or inside (E, G, and I) of A549 cells. 0.1 mg/ml Avr1b(FL)-GFP was incubated with 0.1 mg/ml biosensor at 2°C for 2 hr (D, F, and H) or 37°C for 8 hr (E, G, and I) then washed twice. Light micrograph (panel 1); GFP image (panel 2); mCherry image (panel 3); overlay (panel 4). The scale bars represent 10 μm.

(J–L) Colocalization of indicated GFP fusions with FM4-64. A549 cells were incubated with GFP fusion protein (0.1 mg/mL) for 2.5 min at 37°C, in the presence of 5 μM FM4-64, then washed. Light micrograph (panel 1); GFP image (panel 2); FM4-64 image (panel 3); overlay (panel 4). The scale bar represents 5 μm. See also Figure S5U, which shows FM4-64 entry alone.

depletes the surface of binding sites (based on the binding curves, nearly 90% of the binding sites are occupied at the protein concentrations used), bringing uptake to a temporary halt and resulting in a loss of fluorescence as the internalized GFP was degraded; accumulation presumably resumed only after PI3P was restored to the cell surface. This pattern resembles the endocytosis-mediated loss of cell surface receptors triggered by many ligands.

To test the role of endocytosis in effector-GFP accumulation, we measured the effect of compounds which inhibit several forms of endocytosis. Accumulation of Avr1b- and AvrL567-GFP fusions was inhibited by the phosphatidylinositol-3-kinase (PI3K) inhibitor wortmannin, that inhibits both clathrin-mediated endocytosis and PI3P biosynthesis, and by two inhibitors of lipid raft-mediated endocytosis, nystatin and filipin (Figure 6F and Figure S6A). Tyrphostin A23, N-ethylmaleimide, and LY294002, that inhibit clathrin-mediated endocytosis, and cytochalasin D, that inhibits macropinocytosis, did not inhibit accumulation (Figure 6F and Figure S6A). Although a high background fluorescence was observed in the presence of nystatin and filipin, no localized binding or entry of protein could be observed microscopically (Figure 6K and Figure S6D), suggesting that disruption of lipid rafts had disrupted the distribution of PI3P on the cell surface. To examine if wortmannin was acting by inhibiting endocytosis per se, or by depleting the cell surface of PI3P, A549 cells were preincubated for different periods of time with wortmannin. The longer that the cells were preincubated with wortmannin, the less effector-GFP protein entered, even at 2.5 min (Figure 6H and Figure S6B), suggesting that cell surface PI3P was becoming depleted during the preincubation. This was confirmed by measuring binding of the effectors and a PI3P biosensor at 2°C after 6 hr preincubation (Figure 6J). When the cells were only partially depleted of PI3P (by 30 or 60 min preincubation) entry of the effectors resumed after one hour as normal (Figure 6F), suggesting that endocytosis itself was unaffected. Binding and entry by the synthetic cell entry fusion Arg9-GFP was unaffected by wortmannin, nystatin or filipin, indicating that the action of these inhibitors was specific. Entry of Arg_9-GFP was instead inhibited by the macropinocytosis inhibitor cytochalasin D (Figures 6G and 6I), as reported previously for plant cells (Chang et al., 2007). Entry of Avr1b(FL)-GFP and AvrL567(N)-GFP into soybean root suspension culture cells was inhibited completely by filipin and partially by nystatin (Figure 6L and Figure S6E), indicating that lipid rafts are also required for PI3P-mediated entry into plant cells.

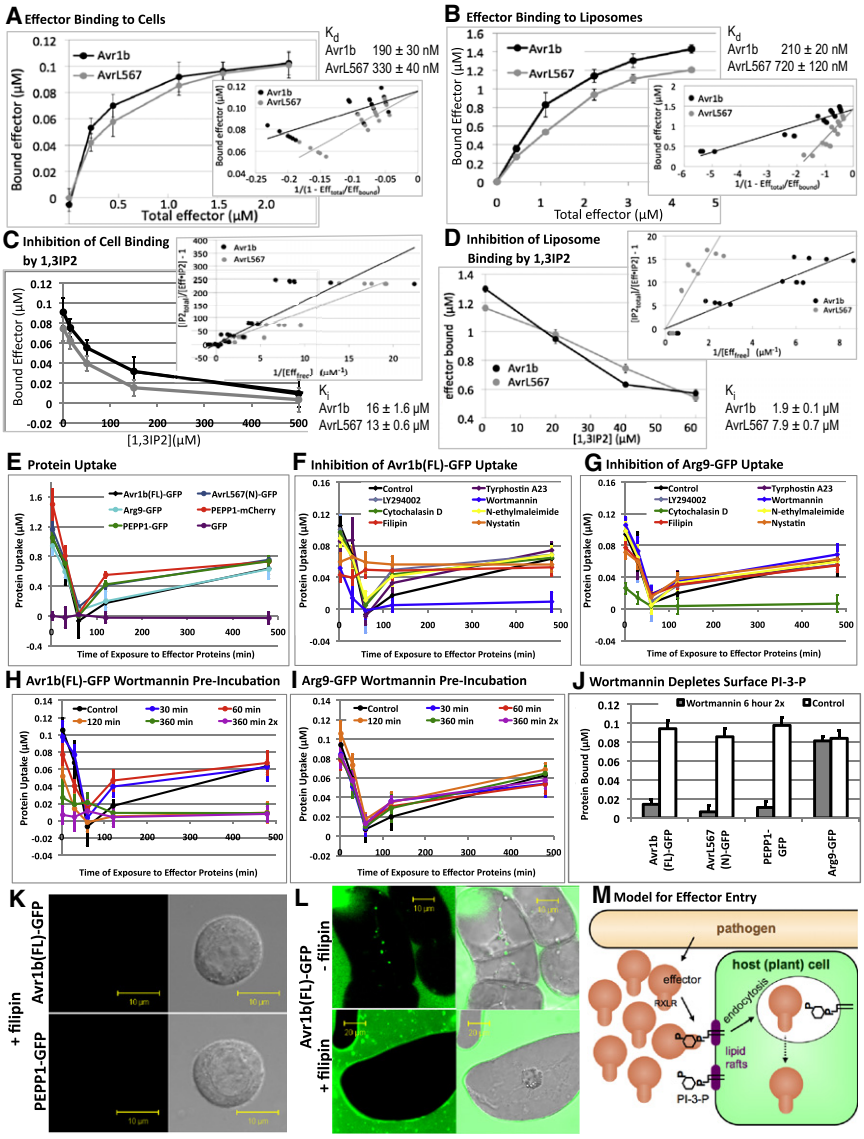

Figure 6. Mechanism of Binding and Entry of Effectors into Host Cells

Error bars in all panels indicate standard errors from four to six replicates.

(A and B) Quantitation of binding of Avr1b and AvrL567 to A549 cells (A) and PI3P-containing liposomes (B). Error bars indicate standard errors. Insets show plots of individual replicate data points used to estimate dissociation constants (K_d's).

(C and D) Quantitation of inhibition by 1,3IP2 of binding of Avr1b and AvrL567 to A549 cells (C) and PI3P-containing liposomes (D). Insets show plots of individual replicate data points used to estimate inhibition constants (K_i's).

(E) Kinetics of accumulation of effector fusions and biosensors in A549 cells.

(F and G) Inhibition of Avr1b(FL)-GFP (F) and Arg9-GFP accumulation at 37°C by endocytosis inhibitors. Inhibitors were added 2 hr before the proteins. See also Figure S6.

(H and I) Inhibition of Avr1b(FL)-GFP (F) and Arg9-GFP accumulation at 37°C by preincubation with wortmannin for different times. "360 min 2×" indicates two Wortmannin additions (at 0 and 180 min). Figure S6B shows data for AvrL567.

(J) Depletion of surface PI3P by incubation for 6 hr at 37°C with Wortmannin additions at 0 min and 180 min.). Binding was assayed at 2°C.

(K) Elimination of effector and biosensor binding sites on A549 cells by incubation with filipin for 2 hr. Binding was assayed at 2°C. Fluorescent images (left panels); overlays (right panels). Figure S6D shows additional photographs for PEPP1, Avr1b and AvrL567, and for nystatin.

(L) Entry of Avr1b(FL)-GFP into soybean root suspension cultures and inhibition by filipin. Cells were exposed to the protein (1.0 mg/mL) for 8 hr at 25°C, then photographed without washing. Note labeling of vesicles in the absence of filipin. Fluorescent images (left panels); overlays (right panels). See also Figure S6E.

(M) Proposed model for effector entry. Binding of effectors via their RXLR domains to PI3P, possibly located in lipid rafts, leads to entry by endocytosis. The mechanism of escape from endosomes is currently unknown. The moderate affinity of the effectors for PI3P facilitates binding on the outer surface but dissociation from PI3P inside the cell.

DISCUSSION

Domains containing RXLR and dEER motifs are responsible for entry of oomycete effector proteins into host plant cells (Dou et al., 2008; Grouffaud et al., 2008; Whisson et al., 2007). Entry of effector proteins into plant cells does not require the presence of the pathogen (Dou et al., 2008). We extend these findings here with similar experiments with full-length Avr1b protein and with two additional oomycete effectors, Avh331 and Avh5. Furthermore, our results with effectors from three fungal pathogens, AvrL567, AvrLm6 and Avr2, suggest that these effectors also can enter plant cells independently of the pathogen, mediated by RXLR-like motifs, though future, in planta experiments with fungal transformants would need to confirm the role of the RXLR-like motifs.

Our results show that all effectors (oomycete and fungal) could bind with high affinity only to PI3P and/or PI4P, via RXLR motifs, but not to other PI-polyphosphates or any anionic phospholipids tested. Thus, binding is very specific and not simply an electrostatic interaction with positive charges of the arginine residues (Langel, 2006). The affinity of binding of Avr1b and AvrL567 to PI3P in liposomes was comparable to those of characterized PI3P-binding proteins, yet the primary structures of the RXLR-dEER effector domains do not resemble any known phosphoinositide binding domains (Lemmon, 2008).

We identified PI3P on the surface of both soybean roots cells and human A549 cells using three structurally different PI3P-specific biosensors, but it was absent from the surface of erythrocytes. It remains to be determined whether the majority of animal cell types have PI3P on their surface, or whether this

Protein	Sequence	Lipid binding PI-3-P	Lipid binding PI-4-P	Leaf Cell Entry	Root Cell Entry	Human Cell Entry	Inhibition
Avr1b(FL)	|TEYSDETNIAMVESPDLVRRSLRNGDIAGGRFLRAHEEDDAGERTFSVTD...	+	+	1.00	Y	Y	Y
Avr1b(FL)rxlr^{rflr-}	|TEYSDETNIAMVESPDLVRRSLRNGDIAGGQFLRAHEEDDAGERTFSVTD...	–	–	0.00	N	N	nt
Avr1b(FL)deer^{-}	|TEYSDETNIAMVESPDLVRRSLRNGDIAGGRFLRAHAAAAAGAATFSVTD...	+	+	0.00	N	Y	nt
Avr1b(N)	|TEYSDETNIAMVESPDLVRRSLRNGDIAGGRFLRAHEEDDAGERTFSVTD|	–	+	1.00	Y	Y	Y
Avr1b(N) rxlr^{-}	|TEYSDETNIAMVESPDLVRAAAANGDIAGGAAAAAHEEDDAGERTFSVTD|	–	–	0.00	N	N	nt
Avr1b(N) deer^{-}	|TEYSDETNIAMVESPDLVRRSLRNGDIAGGRFLRAHAAAAAGAATFSVTD|	–	–	0.00	N	N	nt
Avr1b(N) rflr^{rflr}	|TEYSDETNIAMVESPDLVRRSLRNGDIAGGFRLRAHEEDDAGERTFSVTD|	–	–	0.00	N	N	nt
Avr1b(N) rflr^{rfrl}	|TEYSDETNIAMVESPDLVRRSLRNGDIAGGRFRLAHEEDDAGERTFSVTD|	–	–	0.00	N	N	nt
Avr1b(N) rflr^{qflr}	|TEYSDETNIAMVESPDLVRRSLRNGDIAGGQFLRAHEEDDAGERTFSVTD|	–	–	0.00	N	N	nt
Avr1b(N) rflr^{fyr}	|TEYSDETNIAMVESPDLVRRSLRNGDIAGGRFYRAHEEDDAGERTFSVTD|	–	+	0.84	Y	Y	nt
Avh331(N,FL)	|LTCATSEQQTRPELCFFFSVRSSWPSTISDGACLALVSAEQGATAGRNT LSLRSMMATEDMATSTRSLRSQATNVDDDANVSIENRGM|	+	+	1.07	Y	nt	Y
Avh331(N,FL)rslr^{-}	|LTCATSEQQTRPELCFFFSVRSSWPSTISDGACLALVSAEQGATAGRNT LSLRSMMATEDMATSTAAAASQATNVDDDANVSIENRGM|	–	–	0.00	N	nt	nt
Avh331(N) deer^{-}	|LTCATSEQQTRPELCFFFSVRSSWPSTISDGACLALVSAEQGATAGRNT LSLRSMMATEDMATSTRSLRSQATNVAAAANVSIANAGM|	–	–	0.00	N	nt	nt
Avh5(N,FL)	|TRVPDDANLQSVNAPVQTVTRSRRFLRTADTDIVYEPKVHNPGK|	+	–	nt	Y	nt	nt
Avh5(N,FL) rslr^{-}	|TRVPDDANLQSVNAPVQTVTRSRAAAATADTDIVYEPKVHNPGK|	–	–	nt	N	nt	nt
Avh5(N,Fl) deer^{-}	|TRVPDDANLQSVNAPVQTVTRSRRFLRTAATAIVYAPAVHNPGK|	–	–	nt	N	nt	nt
AvrL567(N)	|MEHVPAELTRVSEGYTRFYRSPTASVILSGLVKVKWDNEQMTMP|	+	±	0.70	Y	Y	Y
AvrL567(N) rfyr^{-}de^{-}	|MEHVPAELTRVSEGYTAAAASPTASVILSGLVKVKWANAQMTMP|	–	–	0.00	N	N	nt
AvrLm6(N)	|ESGRRDGVDDTRTLKVVKGTGGRFVFSSRYWTKAEGAPHEG|	+	+	0.95	Y	Y	Y
AvrLm6(N) RTLK^{qnvq}	|ESGRRDGVDDTQAVQVVKGTGGRFVFSSRYWTKAEGAPHEG|	+	+	0.95	Y	Y	nt
AvrLm6(N) rywt^{tvvq}	|ESGRRDGVDDTRTLKVVKGTGGRFVFSSQVVQKAEGAPHEG|	-	-	0.00	N	N	nt
Avr2(N)	|LPVEDADSSVGQLQGRGNPYCVFPGRRTSSTSFTTSFSTEP LGYARMLHRDPPYERAGNSGLNHRIYERSR|	+	+	0.93	Y	Y	Y
Avr2(N) RMLHRD^{qvvnqn}	|LPVEDADSSVGQLQGRGNPYCVFPGRRTSSTSFTTSFSTEPLGYA QVVNQNPPYERAGNSGLNHRIYERSR|	+	+	0.89	Y	Y	nt
Avr2(N) riyer^{qvvqq}	|LPVEDADSSVGQLQGRGNPYCVFPGRRTSSTSFTTSFSTEPLGYA RMLHRDPPYERAGNSGLNHQVVQQSR|	-	-	0.00	N	N	nt
PfHRPII(N)	|FNNNLCSKNAKGLNLNKRLLHETQAHVDDAHHAHHVAD|	+	+	1.15	Y	Y	nt
PfHRPII(N) pexel^{-}	|FNNNLCSKNAKGLNLNKAAAAATQAHVDDAHHAHHVAD|	+	–	nt	N	N	nt
Arg9	|RRRRRRRRR|	±	±	1.13	Y	Y	N

Figure 7. Summary of Amino Acid Sequences and Cell Entry Activities of Effector Fusions and Mutants

Active and inactive RXLR-like motifs are blue and green respectively; dEER motifs, active residues are in red. (N) indicates N-terminal region only; (FL) indicates full-length protein; (N,FL) indicates identical results for N-terminal regions and full-length proteins. Leaf cell entry measured by particle bombardment. Lipid binding and root cell and human cell uptake are described qualitatively. Inhibition indicates whether protein entry into roots and A549 cells was blocked by the three PI3P-binding biosensors, 1,3IP2 and 1,4IP2 (in no case did the results differ among the two cell types and five inhibitors). Lipid binding measured by filter and liposome assays; +, strong; ±, weak; –, none; Y, yes; N, no; nt, not tested. See also Figure S7.

is restricted to certain cell types, such as epithelial cells. The presence of RXLR-dEER motif effectors in oomycete pathogens of a broad diversity of plants (Rehmany et al., 2005; Tyler et al., 2006; Jiang et al., 2008) suggests that cell surface PI3P should be widely present in plants, but this remains to be directly tested.

In aggregate, our data strongly support the hypothesis that RXLR-mediated binding to PI3P mediates entry of oomycete and fungal pathogen effectors into plant cells. The functional connection between PI3P binding and plant cell entry is underlined by the observation that all RXLR mutations that abolish PI3P binding also abolish cell entry (12 mutations in 9 effectors) and all RXLR mutations that fail to abolish PI3P binding also fail to abolish cell entry (3 mutations in 3 effectors) (Figure 7). Similar findings with the human A549 cells suggest the possibility that oomycetes and fungi that infect humans and other animals could utilize effectors that enter host cells via PI3P binding.

Our data on localization of the effector-GFP fusions shortly after their exposure to human cells and to soybean suspension culture cells, together with the effects of specific endocytosis inhibitors, support the hypothesis that the effectors enter both plant and animal cells via lipid raft-mediated endocytosis (Figure 6M). The K_d's of Avr1b and AvrL567 for PI3P are well above the threshold required for attachment to PI3P-containing intracellular membranes (must be less than 5–7 nM; Blatner et al., 2004), suggesting that oomycete and fungal effectors should readily release from PI3P-containing membranes once inside the host cell (Figure 6M), leaving them free to target a wide variety of host cellular compartments. A variety of bacterial toxins also enter host cells via lipid raft-mediated endocytosis following binding to a lipid receptor, most commonly a glycolipid (Lafont et al., 2004; Lord et al., 1999). The protein toxin PtrToxA from *Pyrenophora tritici-repentis*, enters via an RGD vitronectin-like adhesion motif, probably via receptor-mediated endocytosis (Sarma et al., 2005). The mechanism by which the RXLR effectors escape from endosomes is unknown. Bacterial toxins escape via several mechanisms including retrograde translocation from the ER and transit of partially unfolded proteins directly across membranes (Lafont et al., 2004; Lord et al., 1999). Although we observed that *Plasmodium* effectors also bound PI3P, and did so via their Pexel motif, the role of PI3P in the entry of *Plasmodium* effectors into erythrocytes across the parasitiphorous vacuolar membrane must be different than its role in oomycete and fungal effector translocation, since the Pexel motifs are cleaved within the parasite endoplasmic reticulum (Chang et al., 2008) and transported into the erythrocyte via a pathogen-derived translocon (de Koning-Ward et al., 2009; Maier et al., 2008). Perhaps PI3P binding is required for correct cleavage and targeting. Phosphoinositide levels are strongly elevated in *Plasmodium*-infected erythrocytes due to export of parasite phosphatidylinositol-3-kinase into the erythrocyte cytoplasm (Vaid et al., 2010). We do not know if oomycete or fungal RXLR motifs are ever cleaved, for example as part of the mechanism for escaping endosomes.

Our data demonstrate that effectors from diverse fungal plant pathogens, as well as oomycetes, utilize RXLR-mediated PI3P-binding to enter plant cells. The fungal pathogens include an obligately biotrophic basidiomycete that forms haustoria (*M. lini*; AvrL567), a xylem-dwelling ascomycete vascular wilt

pathogen (*F. oxysporum* f.sp. *lycopersici*; Avr2) and a hemibiotrophic ascomycete leaf and stem pathogens that remains confined to the apoplast (*L. maculans*; AvrLm6). Thus PI3P-mediated effector entry may have evolved independently in several lineages of fungi as well as in the oomycetes.

Our mutagenesis survey of the Avr1b RXLR motif and the diverse functional motifs found in the fungal effectors together suggest that a wide diversity of RXLR-related sequences may support cell entry via PI3P-binding. Bioinformatic screens with the highly redundant motif suggested by our data ([RHK]X[LMIFYW]) identify huge numbers of matches, most of which are likely spurious as judged by searches of permuted protein sequences (R. Jiang and B.M.T., unpublished data), and by the presence of inactive motifs in Avr1b, Avh331, AvrLm6, and Avr2 (Figure 7). Thus, it is very likely that there are additional requirements for cell entry, as noted by Bhattacharjee et al., (2006) and Dou et al. (2008). Biochemical screening for phosphoinositide binding will however provide a powerful tool for screening or directly isolating new candidate effector proteins from all classes of microbes. It may also enable detection of phosphoinositide-binding plant or animal proteins that can traffic through intercellular spaces and enter into target cells to transduce signals. Presumably cell surface PI3P plays a role in the normal physiology of plants and animals.

Understanding the role of phosphoinositides in pathogen effector entry also opens the possibility of targeting cell entry domains or external phosphoinositides for preventative or therapeutic intervention in both agriculture and medicine. The finding that PI3P-binding proteins and IP2 can block effector entry into both plant and human cells provides a proof-of-concept for this approach.

EXPERIMENTAL PROCEDURES

Plasmid Construction

Cloning strategies for all plasmids and the primers are reported in the Extended Experimental Procedures and in Table S3, Table S4, Table S5, and Table S6.

Protein Expression in *E. coli*

E. coli cells containing plasmids encoding each fusion protein were grown at 37°C to an OD_{600} of 0.6. Protein expression was induced with 1–5 mM IPTG and cell growth was continued at 16°C to 37°C for 1.5–16 hr depending on the protein (see Extended Experimental Procedures).

Purification of His-tagged GFP Fusion Proteins

Cells were lysed by sonication then the fusion proteins were collected from the supernatant using a Ni-NTA column (QIAGEN). Pooled fractions were concentrated and equilibrated to the appropriate assay buffer using a Amicon concentrator, and the purity was assessed by gel electrophoresis (Figure S7). See Extended Experimental Procedures for additional details.

Purification of GST-Fusion Proteins

GST fusion proteins were collected from the supernatant using glutathione-sepharose 4B beads (GE Healthcare). Where necessary, the GST tag was removed by digestion with thrombin. See Extended Experimental Procedures for additional details.

Lipid Filter-Binding Assays

Lipids were dissolved in chloroform: methanol: water (65:30:8) then spotted at appropriate concentrations onto membranes. Membranes were incubated in blocking buffer for 1 hr, then the probe protein (20 μg) was added and incubation continued overnight at 4°C. After washing, bound proteins were detected with rabbit anti-GFP or goat anti-GST antibody followed by an HRP-secondary antibody conjugate. Detection was carried out using ECL reagent. See Extended Experimental Procedures for additional details.

Liposome-Binding Assays

Liposomes were prepared from a suspension of PC, PE, and where appropriate a PI-x-P, in chloroform/methanol/water (65:30:8). Lipid mixtures were dried then rehydrated by three cycles of freeze/thawing. Large unilamellar vesicles were formed by extruding the lipid suspension through a 0.1 μM filter. After precentrifugation, protein was added to liposomes and incubated for 1 hr at room temperature. If needed 1,3IP2 or 1,4IP2 were incubated with the proteins for 30 min at room temperature before addition to the liposomes. Protein-liposome mixtures were centrifuged at 100,000 g for 15 min at 25°C. Pellets containing liposome-bound proteins and supernatants containing free proteins were then analyzed by SDS-PAGE. See Extended Experimental Procedures for additional details.

Soybean Root and Suspension Culture Protein Uptake Assays

1.5 cm root tips were cut from vermiculite-grown seedlings and placed into the effector or biosensor protein solution (1 mg/mL protein) and incubated for 12–15 hr at 28°C. For inositol diphosphate inhibition assays, the protein was preincubated with 500 μM 1,3IP2 or 1,4IP2 for 30 min at room temperature before the addition of root tips. For inhibition tests with biosensor proteins, the root tips were preincubated for 3 hr at room temperature in biosensor protein (5 mg/ml) before addition of the effector. After uptake, the root tips were washed in 75 ml of water for 2 hr. For assays with soybean root cell suspension cultures, effector-GFP fusion proteins (100 μg/ml) were incubated with 3 day old cultures for 6 hr at 25°C or at 2°C for 12 hr then photographed without washing. Filipin (50 μg/mL) and nystatin (50 μg/mL) were added 2 hr prior to protein addition. See Extended Experimental Procedures for additional details, including the confocal microscopy.

Human Cell Uptake Assays

Human A549 cells in a 96-well plate were cultured in 90 μl DMEM, 0.1% FBS (DMEM/FBS) at 37°C. Fusion protein was added to each well and incubated at 37°C for 2.5 min to 9 hr, as indicated, or at 2°C for 2 hr. Cells were washed twice and then suspended in 0.25% trypsin and photographed. Where used, the following were dissolved in DMSO and added to cells to final concentrations of: FM4-64, 5 μM; wortmannin, 1 μM; LY249002, 1 μM; tyrphostin A23, 350 μM; N-ethylmaleimide, 1 mM; cytochalasin D, 10 μM, filipin 50 μg/mL, nystatin 50 μg/mL. FM4-64 was added with the protein; the inhibitors were added 2 hr beforehand except where stated otherwise.

To assay inhibition by inositol diphosphate, effector fusion protein was preincubated with 1,3IP2 or I,4IP2 (1 mM) for 30 min at room temperature then added to an equal volume of cells. For inhibition assays, biosensor proteins (0.1 mg/mL) were incubated with the cells for 3 hr at 37°C before addition of effector protein. For dual staining, equal concentrations of the two proteins were added simultaneously to the cells. In all cases, the cells were incubated at 37°C a further 8–9 hr after effector addition (as indicated), then washed and photographed as described in the Extended Experimental Procedures.

To quantitate binding and uptake, GFP fluorescence was measured in the 96-well plates using a microplate spectrofluorometer. Four to six replicates were used, and 20 scans were averaged per replicate. A standard curve in the linear range of detection (0–100 μg/mL) was used to convert emission into protein concentration. See Extended Experimental Procedures for additional details.

Estimation of Binding and Inhibitor Constants

Binding constants and their standard errors were estimated by using the LINEST function of Microsoft Excel to fit a straight line to a plot of: E_b versus $P_t + K_d/(1-E_t/E_b)$ where E_b = [bound effector], E_t = [total effector], P_t = [available PI3P target] (the intercept), and K_d = the dissociation constant (the gradient). The number of PI3P molecules per cell was estimated from P_t. To estimate the inhibition constants and their standard errors for 1,3IP2, a straight line through the origin was fitted to a plot of I_t/EI - 1 versus K_i/E_f where E_f = [free effector] = $K_d/(P_t/E_b - 1)$, I_t = [total inhibitor], EI = [effector-inhibitor complex] = $E_t - E_b - E_f$ and K_i = the inhibition constant (the gradient). See Extended Experimental Procedures for additional details.

SUPPLEMENTAL INFORMATION

Supplemental Information includes Extended Experimental Procedures, Supplemental References, seven figures, and six tables and can be found with this article online at doi:10.1016/j.cell.2010.06.008.

ACKNOWLEDGMENTS

The project was conceived by B.M.T, W.S., and D.D., and the experiments were planned by all authors. S.D.K. and B.G. conducted most of the experiments with contributions from D.G.S.C., D.D., E.F., A.C., R.H., and F.A. S.D.K and B.M.T wrote the paper with input from all authors. We thank Furong Sun and Vincenzo Antignani for technical assistance; Rays Jiang (Broad Institute) for bioinformatics assistance; John McDowell, Ryan Anderson (Virginia Tech), and Frank Takken (University of Amsterdam) for useful discussions; Joop Vermeer and Teun Munnik (University of Amsterdam) for the Hrs-2xFYVE biosensor gene; Michael Klemba (Virginia Tech) for human erythrocytes, Saghai Maroof (Virginia Tech) for soybean seed and Maureen Lawrence, Lisa Gunderman and Emily Alberts for manuscript preparation. This work was supported by the National Research Initiative of the USDA National Institute of Food and Agriculture, grant number #2007-35319-18100 (to B.M.T), by the U.S. National Science Foundation, grant number IOS-0924861 (to B.M.T), in part by the 973 program of the Ministry of Science and Technology of China, grant #2006CB101901 and by grant 15 from the Earmarked Fund for Modern Agro-industry Technology Research System of China (to W.S.). S.D.K. was supported in part by a U.S. National Science Foundation predoctoral fellowship and B.G. was supported by a China Scholarship Council fellowship, #2007U27066, via NW A & F University.

Received: August 20, 2009
Revised: March 30, 2010
Accepted: May 10, 2010
Published: July 22, 2010

REFERENCES

Armstrong, M.R., Whisson, S.C., Pritchard, L., Bos, J.I., Venter, E., Avrova, A.O., Rehmany, A.P., Bohme, U., Brooks, K., Cherevach, I., et al. (2005). An ancestral oomycete locus contains late blight avirulence gene Avr3a, encoding a protein that is recognized in the host cytoplasm. Proc. Natl. Acad. Sci. USA *102*, 7766–7771.

Bhattacharjee, S., Hiller, N.L., Liolios, K., Win, J., Kanneganti, T.D., Young, C., Kamoun, S., and Haldar, K. (2006). The malarial host-targeting signal is conserved in the Irish potato famine pathogen. PLoS Pathog *2*, e50.

Bhavsar, A.P., Guttman, J.A., and Finlay, B.B. (2007). Manipulation of host-cell pathways by bacterial pathogens. Nature *449*, 827–834.

Blatner, N.R., Stahelin, R.V., Diraviyam, K., Hawkins, P.T., Hong, W., Murray, D., and Cho, W. (2004). The molecular basis of the differential subcellular localization of FYVE domains. J. Biol. Chem. *279*, 53818–53827.

Boon, J.M., and Smith, B.D. (2002). Chemical control of phospholipid distribution across bilayer membranes. Med. Res. Rev. *22*, 251–281.

Chang, H.H., Falick, A.M., Carlton, P.M., Sedat, J.W., Derisi, J.L., and Marletta, M.A. (2008). N-terminal processing of proteins exported by malaria parasites. Mol. Biochem. Parasitol. *160*, 107–115.

Chang, M., Chou, J.C., and Lee, H.J. (2005). Cellular internalization of fluorescent proteins via arginine-rich intracellular delivery peptide in plant cells. Plant Cell Physiol. *46*, 482–488.

Chang, M., Chou, J.C., Chen, C.P., Liu, B.R., and Lee, H.J. (2007). Noncovalent protein transduction in plant cells by macropinocytosis. New Phytol. *174*, 46–56.

Chisholm, S.T., Coaker, G., Day, B., and Staskawicz, B.J. (2006). Host-microbe interactions: shaping the evolution of the plant immune response. Cell *124*, 803–814.

de Koning-Ward, T.F., Gilson, P.R., Boddey, J.A., Rug, M., Smith, B.J., Papenfuss, A.T., Sanders, P.R., Lundie, R.J., Maier, A.G., Cowman, A.F., and Crabb, B.S. (2009). A newly discovered protein export machine in malaria parasites. Nature *459*, 945–949.

Dou, D., Kale, S.D., Wang, X., Jiang, R.H.Y., Bruce, N.A., Arredondo, F.D., Zhang, X., and Tyler, B.M. (2008). RXLR-mediated entry of Phytophthora sojae effector Avr1b into soybean cells does not require pathogen-encoded machinery. Plant Cell *20*, 1930–1947.

Dowler, S., Currie, R.A., Campbell, D.G., Deak, M., Kular, G., Downes, C.P., and Alessi, D.R. (2000). Identification of pleckstrin-homology-domain-containing proteins with novel phosphoinositide-binding specificities. Biochem. J. *351*, 19–31.

Ellis, J., Catanzariti, A.M., and Dodds, P. (2006). The problem of how fungal and oomycete avirulence proteins enter plant cells. Trends Plant Sci. *11*, 61–63.

Ellis, J.G., Dodds, P.N., and Lawrence, G.J. (2007). Flax rust resistance gene specificity is based on direct resistance-avirulence protein interactions. Annu. Rev. Phytopathol. *45*, 289–306.

Fudal, I., Ross, S., Gout, L., Blaise, F., Kuhn, M.L., Eckert, M.R., Cattolico, L., Bernard-Samain, S., Balesdent, M.H., and Rouxel, T. (2007). Heterochromatin-like regions as ecological niches for avirulence genes in the Leptosphaeria maculans genome: map-based cloning of AvrLm6. Mol. Plant Microbe Interact. *20*, 459–470.

Grouffaud, S., van West, P., Avrova, A.O., Birch, P.R., and Whisson, S.C. (2008). Plasmodium falciparum and Hyaloperonospora parasitica effector translocation motifs are functional in Phytophthora infestans. Microbiology *154*, 3743–3751.

Hiller, N.L., Bhattacharjee, S., van Ooij, C., Liolios, K., Harrison, T., Lopez-Estrano, C., and Haldar, K. (2004). A host-targeting signal in virulence proteins reveals a secretome in malarial infection. Science *306*, 1934–1937.

Houterman, P.M., Ma, L., van Ooijen, G., de Vroomen, M.J., Cornelissen, B.J., Takken, F.L., and Rep, M. (2009). The effector protein Avr2 of the xylem-colonizing fungus Fusarium oxysporum activates the tomato resistance protein I-2 intracellularly. Plant J. *58*, 970–978.

Jia, Y., McAdams, S.A., Bryan, G.T., Hershey, H.P., and Valent, B. (2000). Direct interaction of resistance gene and avirulence gene products confers rice blast resistance. EMBO J. *19*, 4004–4014.

Jiang, R.H.Y., Tripathy, S., Govers, F., and Tyler, B.M. (2008). RXLR effector reservoir in two Phytophthora species is dominated by a single rapidly evolving super-family with more than 700 members. Proc. Natl. Acad. Sci. USA *105*, 4874–4879.

Jones, J.D., and Dangl, J.L. (2006). The plant immune system. Nature *444*, 323–329.

Kale, S.D., and Tyler, B.M. (2009). Assaying effector function in planta using double-barreled particle bombardment. In Methods in Molecular Biology The Plant Immune Response, J.M. McDowell, ed. (Totowa, NJ: Humana).

Khang, C.H., Berruyer, R., Giraldo, M.C., Kankanala, P., Park, S.-Y., Czymmek, K., Kang, S., and Valent, B. (2010). Translocation of *Magnaporthe oryzae* effectors into rice cells and their subsequent cell-to-cell movement. Plant Cell *22* 10.1105/tpc.1109.069666.

Lafont, F., Abrami, L., and van der Goot, F.G. (2004). Bacterial subversion of lipid rafts. Curr. Opin. Microbiol. *7*, 4–10.

Langel, U. (2006). Handbook of cell-penetrating peptides, Second Edition (Boca Raton, FL: CRC / Taylor & Francis).

Lee, S.A., Kovacs, J., Stahelin, R.V., Cheever, M.L., Overduin, M., Setty, T.G., Burd, C.G., Cho, W., and Kutateladze, T.G. (2006). Molecular mechanism of membrane docking by the Vam7p PX domain. J. Biol. Chem. *281*, 37091–37101.

Lemmon, M.A. (2008). Membrane recognition by phospholipid-binding domains. Nat. Rev. Mol. Cell Biol. *9*, 99–111.

Lord, J.M., Smith, D.C., and Roberts, L.M. (1999). Toxin entry: how bacterial proteins get into mammalian cells. Cell. Microbiol. *1*, 85–91.

Lou, Y., Ma, H., Lin, W.H., Chu, Z.Q., Mueller-Roeber, B., Xu, Z.H., and Xue, H.W. (2006). The highly charged region of plant beta-type phosphatidylinositol

4-kinase is involved in membrane targeting and phospholipid binding. Plant Mol. Biol. *60*, 729–746.

Maier, A.G., Rug, M., O'Neill, M.T., Brown, M., Chakravorty, S., Szestak, T., Chesson, J., Wu, Y., Hughes, K., Coppel, R.L., et al. (2008). Exported proteins required for virulence and rigidity of *Plasmodium falciparum*-infected human erythrocytes. Cell *134*, 48–61.

Marti, M., Good, R.T., Rug, M., Knuepfer, E., and Cowman, A.F. (2004). Targeting malaria virulence and remodeling proteins to the host erythrocyte. Science *306*, 1930–1933.

Quinn, P.J. (2002). Plasma membrane phospholipid asymmetry. In Subcellular Biochemistry, P.J. Quinn and V.E. Kagan, eds. (London: Kluwer Academic/Plenum Publishers), pp. 39–60.

Rehmany, A.P., Gordon, A., Rose, L.E., Allen, R.L., Armstrong, M.R., Whisson, S.C., Kamoun, S., Tyler, B.M., Birch, P.R., and Beynon, J.L. (2005). Differential recognition of highly divergent downy mildew avirulence gene alleles by RPP1 resistance genes from two Arabidopsis lines. Plant Cell *17*, 1839–1850.

Sarma, G.N., Manning, V.A., Ciuffetti, L.M., and Karplus, P.A. (2005). Structure of Ptr ToxA: an RGD-containing host-selective toxin from Pyrenophora tritici-repentis. Plant Cell *17*, 3190–3202.

Shan, W., Cao, M., Leung, D., and Tyler, B.M. (2004). The *Avr1b* Locus of Phytophthora sojae Encodes an Elicitor and A Regulator Required for Avirulence on Soybean Plants Carrying Resistance Gene *Rps1b*. Mol. Plant Microbe Interact. *17*, 394–403.

Tseng, T.-T., Tyler, B.M., and Setubal, J.C. (2009). Protein Secretion Systems in Bacterial-Host Associations, and their Description in the Gene Ontology. BMC Microbiol. *9*(suppl 1), S2.

Tyler, B.M. (2002). Molecular Basis of Recognition Between *Phytophthora* species and their hosts. Annu. Rev. Phytopathol. *40*, 137–167.

Tyler, B.M. (2007). Phytophthora sojae: root rot pathogen of soybean and model oomycete. Mol. Plant Pathol. *8*, 1–8.

Tyler, B.M. (2009). Entering and breaking: virulence effector proteins of oomycete plant pathogens. Cell. Microbiol. *11*, 13–20.

Tyler, B.M., Tripathy, S., Zhang, X., Dehal, P., Jiang, R.H., Aerts, A., Arredondo, F.D., Baxter, L., Bensasson, D., Beynon, J.L., et al. (2006). Phytophthora genome sequences uncover evolutionary origins and mechanisms of pathogenesis. Science *313*, 1261–1266.

Vaid, A., Ranjan, R., Smythe, W.A., Hoppe, H.C., and Sharma, P. (2010). PfPI3K, a phosphatidylinositol-3 kinase from Plasmodium falciparum, is exported to the host erythrocyte and is involved in hemoglobin trafficking. Blood *115*, 2500–2507.

Vermeer, J.E., van Leeuwen, W., Tobena-Santamaria, R., Laxalt, A.M., Jones, D.R., Divecha, N., Gadella, T.W., Jr., and Munnik, T. (2006). Visualization of PtdIns3P dynamics in living plant cells. Plant J. *47*, 687–700.

Vermeer, J.E., Thole, J.M., Goedhart, J., Nielsen, E., Munnik, T., and Gadella, T.W., Jr. (2009). Imaging phosphatidylinositol 4-phosphate dynamics in living plant cells. Plant J. *57*, 356–372.

Whisson, S.C., Boevink, P.C., Moleleki, L., Avrova, A.O., Morales, J.G., Gilroy, E.M., Armstrong, M.R., Grouffaud, S., van West, P., Chapman, S., et al. (2007). A translocation signal for delivery of oomycete effector proteins into host plant cells. Nature *450*, 115–119.

Note Added in Proof

After this paper was accepted for publication, Rafiqi et al (Plant Cell 10.1105/tpc.109.072983) showed that fungal effectors AvrL567 and AvrM could enter plant cells in a pathogen-independent manner, mediated by RXLR-like sequences, and Murata-Kamiya et al (Cell Host & Microbe DOI 10.1016/j.chom.2010.04.005) showed that a Helicobacter pylori effector CagA enters human cells by binding cell surface phosphatidylserine.